Urol Res (1996) 24:149–160

ORIGINAL PAPER

L. S. Young · M. C. Regan · M. K. Barry
J. G. Geraghty · J. M. Fitzpatrick

Methods of renal blood flow measurement

Received: 16 May 1995 / Accepted: 10 January 1996

Abstract Variations in regional renal blood flow have been implicated in a variety of disease states. Many techniques have been developed in an attempt to accurately assess these changes. The microsphere technique is the most widely used method at the present time. This technique allows focal measurements to be performed, but there is a conflict between the resolution of the method and the number of microspheres necessary in each sample. New imaging techniques such as tomography and autoradiography enable visual assessment of renal blood flow. Though there is no ideal method, these techniques have opened up new possibilities in the quantification of regional renal blood flow.

Key words Regional renal blood flow · Microsphere technique · Tomography · Autoradiography

Introduction

The fundamental importance of the regional distribution of blood flow within the kidney and in particular the division of blood between the cortical and medullary tissue was first recognised by Trueta in 1948 [74]. Subsequent experimental studies have shown regional renal blood flow to be heterogeneous under physiological and a variety of pathophysiological conditions. Relatively small changes in the zonal distribution of renal blood flow may have wide-ranging effects on renal excretory function. While measurement of total renal blood flow is a relatively simple matter, such determinations do not take account of significant alterations in the actual or relative distribution of blood flow at the regional level. Obviously the ability to accurately measure such variation in regional blood flow within the complex structure of the kidney is highly desirable. In this article we review the different techniques available to assess blood flow within this complex organ.

L. S. Young (✉) · M. C. Regan · M. K. Barry · J. G. Geraghty · J. M. Fitzpatrick
Surgical Professorial Unit, Mater Misericordiae Hospital and University College Dublin, Eccles Street, Dublin 7, Ireland

Renal flow and function

The kidney regulates not only the concentrations of metabolic waste products, but also the volume, osmolarity, acid-base status and ionic composition of the extracellular fluid. These functions are mediated via two interdependent regulatory systems, which govern the rate at which the glomerulus filters blood passing through the glomerular tuft and control the rate at which solutes are secreted and reabsorbed along the tubular structures. The quality and regional distribution of renal blood flow is important in this regard.

The kidney receives an extraordinarily high percentage of the total cardiac output (20–25%). This high renal blood flow serves a dual function; primarily it provides blood for filtration, since an adequate glomerular blood supply is necessary if the normal excretory function of the kidney is to be maintained; secondly the renal circulation provides oxygen and nutrients to the renal parenchyma. Alterations in renal blood flow may therefore lead to changes in function not only due to tissue ischaemia, but also as a consequence of changes in glomerular filtration [47].

There is some variation in the exact figures for regional flow provided by the various different methods of measurement of renal blood flow, but there is an overall concordance in terms of the magnitude and pattern of regional distribution.

More than 90% of blood flow entering the kidney goes to supply the renal cortex resulting in a cortical perfusion rate of between 500 and 850 ml/100 g per minute tissue depending on the technique used, while the remainder serves to supply the capsule and the

renal adipose tissue. There does not appear to be any significant difference in the flow to polar and central regions of the cortex. The overall volume of blood passing from the cortex to the medulla is significantly reduced as a result of loss of plasma volume due to filtration in the glomeruli. Measurement of medullary blood flow reveals a flow rate of between 100–250 ml/100 g per minute in the outer and 20–40 ml/min per 100 g in the inner medulla. As observed in the cortex, there does not appear to be any difference in flow between the polar and central regions of the outer medulla.

The low flow rates to the inner medulla, obtained using different techniques, present some problems of interpretation. This arises as a result of the vascular anatomy in this region. It has been suggested that countercurrent exchange between the descending and ascending vasa recta may result in an underestimation of flow using the currently available techniques, since there is no accurate definition of effective blood flow in tissues where countercurrent exchange mechanisms are present. Although these limitations may result in an underestimation of "true" absolute flow, it does not prevent comparative studies from being performed.

The complex anatomy of the kidney has made the accurate determination of its blood flow difficult. Selection of a suitable tracer may mean a compromise between a tracer such as rubidium, which has appreciable diffusion limitations, or iodoantipyrine, which is known to be shunted in the vasa recta. The decision may be made on the basis of areas of interest; for example, cortical blood flow may be examined using a tracer that is shunted in the vasa recta, but will diffuse equally across renal cortical tissue. The vascular architecture of the kidney may also result in axial streaming and geometric exclusion of radiolabelled particles, casting doubt over the accuracy of the microsphere technique. New computer-assisted techniques open up possibilities for looking at regional renal haemodynamics. These techniques rely on intravascular contrast agents or tracers in solution and as a consequence there is no problem with steric hindrance or streaming. However, such tracers may be subject to diffusion limitations and shunting along the vasa recta.

Renal flow and disease states

There are a variety of pathophysiological conditions which alter intrarenal haemodynamics and may thus compromise renal function. Nephrectomy, ureteric obstruction, renal artery stenosis, diabetes and ischaemia and reperfusion injury are among the most important of these. Nephrectomy leads to a sudden decrease in excretory capacity. This in turn initiates a compensatory process which results in hypertrophy of the remnant kidney and a progressive improvement following the acute reduction in renal excretory function [57]. Both partial and complete ureteric obstruction are associated ultimately with a reduction in renal blood flow, which may lead eventually to renal insufficiency of ischaemic aetiology [76]. There is a temporary elevation followed by a sustained reduction in the perfusion of the ipsilateral kidney and a compensatory increase in the perfusion of the contralateral kidney. These changes in total renal blood flow are accompanied by alterations in intrarenal flow, characterised by a shunting of flow from the outer to the inner cortical zones [38, 56, 76]. Renal artery stenosis is well established as a cause of hypertension, ischaemia and renal impairment [21]. Either one or both renal arteries may be occluded. If one is affected, ipsilateral renin production is high while sodium excretion and urine production are low. Contralateral renin production is low. Plasma volume expands and hypertension becomes unresponsive to antiangiotensin agents. If both kidneys are involved and there is no normal contralateral kidney, systemic renin and its production is low, but the plasma volume is expanded and there is hypertension [80]. Diabetes causes impairment of the autoregulation of renal blood flow. Glomerular filtration rate and renal blood flow are increased initially and subsequently fall below normal levels as a result of mesangial hypertrophy, and renal failure ensues [49].

Following a significant period of ischaemia ensued by reperfusion, a marked decrease in glomerular filtration and inner medullary blood flow is seen, with relative preservation of cortical and total renal blood flow [83].

Interpretation of normal renal function has wide-ranging implications beyond the direct consequences on renal parenchyma. The consequences of partial renal damage directly affecting one kidney may also involve the contralateral organ, and other body systems. Accurate assessment of total and regional renal blood flow is therefore imperative in our understanding and treatment of these pathophysiological states.

Total renal blood flow

Total renal blood flow is normally measured by determination of the renal clearance rate of *para*-aminohippuric acid (PAH) or iodopyracet, following low-dose infusion of either compound. Both compounds are ideally suited, since neither compound is metabolised, stored or produced in the kidney, they do not affect renal blood flow and they have a high clearance ratio. Measurement is based on the Fick principle and from the determination of urinary and plasma concentrations the renal clearance can be calculated. This is equal to the effective renal plasma flow since the kidney filters plasma. The actual renal plasma flow and renal blood flow may be calculated as the extraction ratio and haematocrit are known. Using these techniques, human total renal blood flow has been estimated at

approximately 1.1 l/min, which is equal to a total daily renal blood flow of 1640 l/day.

Total renal blood flow may also be measured non-invasively using Doppler ultrasound probes or by more invasive techniques utilising implanted Doppler flow probes or electromagnetic flow transducers. While these techniques give accurate and reproducible determinations of total renal blood flow, they are of limited application in the determination of regional changes in blood flow within the kidney.

Measurement of intrarenal blood flow

Inert-gas methods: ^{85}Kr and ^{133}Xe washout

The Kety inert-gas theory [40] developed by Thornburn [72] in 1963 for measuring blood flow has been used with limited success for the measurement of intrarenal blood flow. This technique is based on the concept of exponential washout of a radioactive inert gas (^{85}Kr or ^{133}Xe) from an organ following injection of the isotope into the arterial inflow. The theory is dependent on the assumption that the rate of accumulation (or dissipation) of an inert substance in the renal parenchyma is proportional to the rate of blood flow, provided that the diffusion constant and the partition coefficient of the gas between tissue and blood are taken into account. An index of organ blood flow may be derived from the equation:

$$F/V_D = K \cdot \lambda/p$$

where F = flow, V_D = volume of distribution of the gas, K = the disappearance rate constant of the gas, λ = partition coefficient of the gas between the tissue and the blood, and p = the specific gravity of the tissue. The externally monitored gas washout curve may be broken into component parts using a "tail subtraction" technique to describe four different flow rates within the kidney [72]. Components I–IV of the multi-exponential decay curve represent flows to the cortex (I), outer medulla (II), inner medulla (III) and perirenal and hilar fat (IV). Previous studies have shown good correlation between component I and cortical blood flow as measured by other techniques, but the limitations of the inert-gas method have cast doubts on the accuracy of components II, III and IV. In particular the measurement of medullary flow with the diffusible gas technique is thought to be impossible due to counter-current exchange and the effect of changing urinary flow on the washout rate [69].

Beyond these difficulties there are several objections to using this technique to measure intrarenal blood flow distribution. There is an inability to ascribe a given anatomical area to a component of the washout curve and furthermore this component may not represent the same area in control and experimental periods. In addition this method measures flow per unit volume, and in situations where the volume may be changing the disappearance rate constant of the gas (K) may be unchanged in the face of significant flow changes [68]. The assumption that the partition coefficient is unaffected by changes in tissue water content has not been tested. Higher flow rates with ^{85}Kr rather than ^{133}Xe, which has a lower partition coefficient, suggest that the same coefficient may not be appropriate for a particular in *vivo* situation [9]. Furthermore, for the disappearance rate constant of the gas (K) to be a function of capillary removal it is assumed that the gas reaches complete equilibrium during the time of the washout curve. If equilibrium fails to occur, K is also a function of the diffusion characteristics of the gas. Studies in skeletal muscle [8] disassociated the disappearance rate of ^{133}Xe from directly measured blood flow during vasodilatation and attributed it to a change in the surface area available for tissue blood exchange. There is recirculation of ^{85}Kr, and this may be an explanation for retardation of ^{85}Kr washout in the cortex [58].

Though it seems doubtful if washout of diffusible inert gases with external detectors can give significant information about intrarenal blood flow distribution, the initial washout rate has been shown to be useful for the assessment of average renal blood flow. The non-invasive inhalation technique using the inert gas ^{133}Xe may prove to be a more successful adaptation of the inert gas method [67].

Hydrogen washout

In order to address the problem of localising the washout component to a particular area using external detection techniques, local detection using implanted electrodes in distinct regions for continuous recording of hydrogen washout rates has been used [6]. This local measurement of hydrogen washout is, however, unable to determine inner medullary blood flow since the efficient exchange of gas in the vasa recta results in the flow of the collecting duct fluid being a major determinant of the medullary washout rate. This effect is thought to be negligible in the outer medulla and cortex.

Other disadvantages of this technique are the potential for changes in renal volume to alter electrode position, the considerable handling of the organ for electrode stabilisation and placement and the unavoidable tissue trauma. Local hydrogen measurement has also failed to confirm the microsphere finding of increased deep cortical flow fraction in vasodilatation [75].

To evaluate the possible flow disturbance due to electrode trauma, Hope et al. [30] have studied the uptake of the inert diffusible tracers ^{131}IAP and tritiated water (THO). They found that in the dog kidney the flow distribution patterns obtained with ^{131}IAP and THO are similar to those obtained with

local hydrogen [4, 75] and ^{85}Kr [58] washout. Moreover, renal vasoconstriction and dilation induced by angiotensin II and acetylcholine, respectively, cause no change in the distribution pattern of ^{131}IAP and THO [14, 15] and therefore the inability of local hydrogen measurement to detect these vasodynamics cannot be blamed on tissue trauma.

Heat diffusion and thermodilution

Heat is another diffusible indicator of intrarenal blood flow distribution analogous to inert gas washout. Accurate interpretation of renal blood flow from heat data is difficult due to a substantial portion of heat being lost through tissue conductivity. Approximately half of the thermal conductivity in the liver is due to blood flow and the other half due to tissue conduction [24]. After an intrarenal artery injection of hot or cold saline, a particular region of the kidney, moving from one steady state temperature to another, ought to follow an exponential function with respect to time. Heat is conducted across the walls of large vessels as well as the capillaries, however, and therefore the tissue adjacent to large vessels is cooler than surrounding tissue. These non-equilibrium redistributions of heat during the early stages of a heat injection contribute rapid disappearance rates to the initial part of the washout curve which have no morphological counterpart. During the final stages of the temperature washout curve, the countercurrent exchange of heat across the arteries and veins in the cortex [60], and the vasa recta in the medulla [3], causes the rate of heat leaving the organ to be delayed. Thus attributing the early and latter parts of the washout curve to anatomical areas is not viable.

A technique using heated thermocouples as a reference to account for perfusion-independent thermal conductivity of the tissue has been somewhat more successful [23]. This method provides important qualitative information about tissue perfusion, but because these methods measure only a single thermal property of a tissue they cannot as yet provide adequate quantitative determination of regional blood flow.

Isotopically labelled iodoantipyrine

Isotopically labelled iodoantipyrine (IAP) is a diffusible tracer which may be used to measure intrarenal blood flow with good accuracy in well-defined anatomical regions. It has the advantage of being non-invasive and there is no reason to suspect that this measuring technique should influence renal blood flow. When the biologically inert tracer is carried to a tissue by arterial blood, the tracer concentration in the tissue (C_1) at time T is determined by the arterial concentration (C_a), the tissue blood partition coefficient [1] and blood flow per unit volume (F/V_1):

$$C_1(T) = \lambda K_1 \, o/^T \, C_a(\exp\{-K_1 T - t\})\,\mathrm{d}t \quad [30]$$

where $K_1 = F/V_1 \cdot l$. Blood flow is estimated by constructing curves for corresponding values of $C_1(T)$ and F/V_1 using arterial concentrations [39]. Accurate assessment of blood flow from a single point on the tissue saturation curve depends on the assumption that instantaneous equilibrium of tracer with venous blood draining any particular region occurs. That is, that each tissue sample, including arteries, capillaries and veins, and the parenchyma itself will behave as an ideal mixing chamber. A correct estimation of the tissue-blood partition coefficient is also essential.

It has been suggested that the uptake of antipyrine in the brain is not determined by blood flow alone, and demonstrates appreciable diffusion limitation at this site [18, 19, 39]. The brain may, however, present a unique position because of the blood-brain barrier. In the myocardium, antipyrine uptake appears to be exclusively flow determined, even at high flow rates. In the kidney, tubular transport and glomerular filtration of IAP may in some small way contribute to diffusion equilibrium. The extent of diffusion limitation in the kidney may be determined by comparison of flow measurements with data obtained by other techniques. Average cortical flow rates utilising IAP [30] are 11% greater than those obtained by measurements of cortical hydrogen desaturation [11]. Total flow rates of up to 30% higher than the average obtained with IAP have, however, been reported [30] using electromagnetic flowmetery, *p*-aminohippuric acid (PAH) clearance and microsphere techniques [2]. This comparison though may be misleading, as these techniques give total flow in millilitres per minute per kidney, and blood flow per gram is obtained by dividing weight determined after the experiment. No correction is made for loss of blood and tissue fluid due to excision and preparation, which may cause an unrealistically high flow rate to be reported. With the IAP method, flow per gram is not affected, as lost fluid is in diffusion equilibrium with the tissue it is draining.

Changes in capillary blood volume influence the degree of tracer equilibrium between tissue and blood. The renal parenchyma has a high capillary blood volume which at any given flow rate increases the transit time of tracer in the tissue and in this manner will enhance its tissue equilibrium.

Blood flow to the inner cortex obtained using IAP is higher than that reported using the microsphere method. The microsphere technique is thought to markedly underestimate deep glomerular flow. Observations that renal vasodilation (with or without increased renal blood flow) will increase the deep microsphere fraction until it approaches IAP flow [4, 14], and that angiotensin II increases the discrepancy between the two methods [15], indicate that there are other contributing factors. Variable net postglomerular capillary

blood flow from superficial to deep layers of the cortex may be influential [4]. This theory is supported by the measurement of the net flow direction of H_2 gas generated locally in the cortex.

The much higher IAP concentration reported in the outer medulla than in deeper layers at the end of infusion periods [30] presents a strong case for countercurrent exchange of IAP between ascending and descending vasa recta. The total medullary blood flow calculated from IAP uptake must therefore be considerably lower than the total inflow of blood to the medulla. The countercurrent exchange effect is to some small extent counteracted by IAP entering the medulla through flow in the loop of Henle. The inflow through the loop is only about a third of total medullary blood flow and the tubular fluid had a much lower IAP concentration due to equilibrium with inner cortical tissue, so therefore it is unlikely that this contribution would fully compensate for the effect of countercurrent exchange.

Rubidium-86 uptake

The distribution and subsequent trapping of isotopic potassium (or rubidium) in different organs constitutes a measure of blood flow distribution [66]. Haring and Pelly [25] in 1956 applied this theory to the determination of medullary blood flow by the ^{86}Rb extraction method.

Blood flow is determined by the equation:

$$M/M_{ref} = F/F_{ref} \quad [36]$$

where M_{ref} is the amount of indicator in the reference blood sample, M the amount of isotope in the specimens and F_{ref} the sampling rate. This technique, as with the transport of inert diffusible gases, measures "effective" or "nutrient" rather than absolute blood flow. A further difficulty with this method is that blood flow may be overestimated in the medulla due to urine contamination, and underestimated in the cortex owing to incomplete extraction. Rubidium is transported to the renal medulla not only by the blood stream but also by the tubular fluid. Originating from the cortex, this rubidium enters the medulla. It is essential that the tubular transport occurring during the sampling time is taken into account when determining medullary blood flow. To examine the extent of this error, Karling et al. [36] looked at the effect of ^{86}Rb transport to the inner medulla. They concluded that urinary contamination is at most 5% within 30 s in the outer medulla, and 1.3% in the inner medulla.

When rubidium is used for estimation of cortical or total renal blood flow, the sampling time should not exceed 5 s, whereas for medullary blood flow a 30-s sampling time is more appropriate [36]. The cellular extraction fraction of rubidium is known to be highly dependent on the flow rate [36, 61, 71]. Microspheres have been administered with rubidium to obtain true total renal blood flow, as the venous effluent of microspheres is very small. Rubidium, however, recirculates within the sampling time, which is critical for cortical blood flow estimations. It is therefore an unsuitable tracer for measurement of blood flow within the cortex. This is of minor importance in the medulla due to the longer transit time and high extraction capacity, making the inflow to the medulla and reference sample almost equal [36].

Rubidium is less diffusible than the inert gases [45] and therefore is not highly dependent on urine flow, nor has it the disadvantage of being shunted between the vasa recta limbs. The 7-s rubidium uptake in the medulla of rats, corresponding to a plasma flow of 0.18 ml/min per gram, is in good agreement with ^{125}I-albumin uptake after correction for a reasonable filtration fraction of juxtamedullary glomeruli, suggesting little countercurrent exchange of rubidium-86 [17]. An additional advantage is that the sampling time is not as critical as it is for other methods, such as labelled albumin, due to rubidium's large volume of distribution [36].

From the current literature it would appear that the rubidium extraction method is suitable for determination of medullary blood flow. Using this technique, Harsing and Pelley [25] have obtained medullary blood flow values similar to those found by Wolgast [81] using ^{32}P-labelled red cells of plasma particles and internal detection. The incomplete extraction of rubidium, however, invalidates the method for cortical blood flow estimations.

Plasma and erythrocyte accumulation and transit time

Labelled plasma and red blood cells may be used as tracers for flow in the inner medulla and papilla. The flow is calculated using the following equation:

$$F_i = V_i/t_i \quad [82]$$

where F_i is the flow of the indicator, V_i the volume of distribution of the indicator within the parenchyma and t_i the mean transit time. Wolgast defined regional red cell volume as the ratio between the equilibrium activity in the tissue and the activity in pure red cells, in a blood sample drawn at the same time. Determination of plasma cell volume is more complicated due to the removal of the chromic phosphate, used for labelling, from the circulation by the liver. Moreover, some of these particles leak out into the extravascular space, adding to the volume determined. Plasma flow volume is therefore determined from indicator dilution curves [82]. To determine the mean transit time, recirculation is corrected to estimate the indicator dilution curve which represents a single circulation. The curve may be divided into two parts by linear log extrapolation. The mean transit time is calculated from the first and major part of the curve, which represents activity passing in

the outer medullary capillary system and activity bound for inner medullary capillary systems passing through the outer medulla in descendent vasa recta. The latter portion represents internal recirculation. There is an inherent error in this method since the time is calculated from approximately three-fourths of the total curve. The time will reflect the passage through a volume which comprises three-fourths of the total volume of distribution. Correction for this error is, however, felt to be unnecessary [82] as red cell volume is also thought to be underestimated due to the non-perfused zone around the detectors. Rasmussen [59] looked at the plasma accumulation curve. He introduced a nearly ideal renal arterial step function in rats using a cross-perfusion technique. Because of the scatter of the data, he concluded that "the early accumulation is likely to follow a curved rather than a straight line". This does not, however, exclude the "initial slope" as a useful indicator for the inner medullary perfusion.

As with all methods of measuring intrarenal blood flow, there are difficulties to be taken into consideration. The trauma from inserting the probe results not only in a damaged zone around the detector surface but also compromises the circulation within the whole monitored volume. Bleeding often occurs in the highly vascularised cortex, though is rarely visible in the medulla. The trauma which results in an underestimation of red cell volume in the cortex may be markedly reduced by introducing the detector into a freely draining performed channel.

The plasma volume is calculated from the area of the first rapid component of the curve. The volume refers not to the real volume, however, but to the volume of distribution of the indicator. If the protein concentration in the vasa recta blood is higher than in the systemic blood, as has been found from micropuncture and microspectrophotometric studies, the calculated values will overestimate true values [73, 79].

Findings of comparatively high plasma volumes in relation to the red cell volumes have been recorded using this technique [82]. Calculation of whole blood flow should therefore take into account the pronounced reduction of red cells found in the inner zone, which indicates red cell skimming, i.e. red cell circuiting between the vasa recta limbs, somewhere in the outer medulla [59, 82].

Measurement of local transit time of labelled plasma and erythrocytes has the advantage of being reproducible and is not affected by the countercurrent exchange at the loop of Henle nor does it suffer from the inaccessibility of microspheres. The trauma associated with this technique, however, limits the use of this method to dogs.

Radionucleotide-labelled microspheres

The microsphere technique is based on the principle that injection into the circulation of particulate matter that is trapped at the level of the capillaries can measure organ blood flow and the distribution of flow within that organ. If the particles are uniformly mixed in the systemic arterial blood, the fraction of blood to an organ or component of an organ is the same as the fraction of the injected particles trapped in the tissue. Therefore if a known amount of particles (Q) are injected into the left ventricle, the quantity of particles (dq) taken up by a piece of tissue during the time interval (dt) is given by the equation:

$$dq = f' \cdot C(t)dt$$

where f' is the flow to the tissue and $C(t)$ is the arterial concentration of the microspheres during the time dt. Taking that the beads are totally extracted by all tissues then:

$$dQ = CO \cdot C(t)dt$$

where dQ is the amount of particles taken up by the entire body during the time dt and CO is the cardiac output. Thus if the total flow, and the total number of particles, are known, the blood flow to any given organ, or organ region, can be determined by the equation:

$$f' = q/Q \cdot CO$$

The general form of the equation is:

$$f' = q/Q_t \cdot F_t$$

where f' is the flow rate to an organ, or region of interest, F_t is the total flow to the organ, or another reference organ, q is the number of particles trapped in the tissue of interest, and Q_t is the total number of particles in the organ or reference organ.

The microsphere technique, derived from this theory, developed by McNay and Abe [50], is based on several assumptions: (1) the microspheres are totally extracted by the tissue in one circulation, (2) they must not damage the tissue of the organ during extraction, (3) they do not alter the blood flow to the organ, or any of its physiological functions and (4) they must be uniformly mixed during injection and have rheological properties similar to those of blood.

For estimation of intrarenal distribution, the cortex is divided into two to four zones parallel to the kidney surface. Microsphere radioactivity is estimated per gram of tissue, giving zonal flow in millilitres per minute per gram. Relative flow fractions may then be calculated from the relative volumes of each zone [5]. Error due to changes in kidney volume after microsphere injection may be corrected for by simultaneous measurement of total renal blood flow [70].

Measurement of intrarenal blood flow using the microsphere technique has been criticised as there is evidence that the spheres may not reach all glomeruli in proportion to blood flow [42]. Axial migration of particles in a flowing stream and geometric exclusion of particles entering branching vessels are known to compromise microsphere distribution.

The flow of blood through a vessel causes red cells to migrate to the centre of the stream, thereby leaving a relatively cell-free area adjacent to the vessel wall, a phenomenon known as axial streaming. When this occurs in the interlobular arteries, a plasma-rich fluid may enter the afferent arterioles of the deep cortex, causing a progressive rise in the haematocrit as the blood reaches the afferent arterioles of the outer cortex. The magnitude of axial streaming increases with the size of the particles relative to the conduit and therefore microspheres considerably larger than red cells are subject to even greater streaming [77]. Katz [37] found that as bead size progressively increased from 10 to 50 μm there is an increasingly disproportionate delivery of microspheres to the outer cortex. He suggested that smaller beads, having less of a streaming artefact, would more closely approximate the true distribution of renal blood flow. Work by Ofstad et al. [52] has shown that microspheres of over 20 μm are trapped before reaching the glomeruli and calculated mean entrance diameters for afferent arterioles and glomerular capillaries of 19.5 and 17.1 μm, respectively.

Microsphere beads smaller than 15 μm, however, have been found to be unsuitable. Using microspheres of 7–10 μm, a substantial shunting of beads through the kidney has been noted which may distort the pattern. Injection of smaller beads has also been associated with hypotension and a reduction in glomerular filtration rate and renal blood flow [37]. Moreover, Archie et al. have demonstrated incomplete trapping of microspheres under 7 μm in lambs and suggested a lower limit of 8 μm in sheep and dogs [1].

Radioactivity is related to sphere volume and this compounds the error due to streaming. Selection of spheres by size therefore influences the amount of radioactivity in a section of the cortex independent of blood flow. For example, a difference in sphere diameter from 15 to 16 μm represents a 20% increase in volume and hence in radioactivity [42]. Comparing the radioactivity distribution of spheres, 12.7 ± 1.2 μm and 8.5 ± 0.8 μm in the outer cortex of rats, Casellas and Mimram found a 12% higher distribution of total radioactivity with the larger spheres than with the smaller ones [10]. Clausen et al. also found significantly different estimates of cortical flow in dogs, using 10-μm and 15-μm spheres [16].

The size and geometry of the preglomerular vessels also influence the distribution of spheres. Afferent arterioles branch from the interlobular artery at right or recurrent angles. This coupled with the small difference in size between sphere and arteriole hinders spheres from entering afferent arterioles. Though many studies indicate that virtually all spheres 15 ± 5 μm in size are trapped in the glomeruli, rather than the preglomerular segments [7, 13, 35, 50, 55], failure of more than 15% of 12.8 ± 1.1-μm spheres to reach the glomeruli in rats has been reported [85]. It is thought that the diameter of commonly used spheres (15 ± 5 μm) and the diameters of the afferent arterioles of experimental animals overlap considerably.

Geometric exclusion will limit the ability of the microsphere technique to determine changes in blood flow distribution. Morkid et al. [52] found that a reduction in arterial pressure leads to a redistribution of large spheres from the outer to the inner cortex. A corresponding redistribution is not seen with small spheres. Heller et al. [28] confirmed this finding using 15-μm spheres and the red cells of chickens. Both workers concluded that the same degree of dilatation of afferent arterioles occurred in all cortical zones. As this artefact is due to geometry, the spheres reaching the dilated arterioles of the deep cortex have a greater chance of entering the deeper glomeruli. The decreased hindrance of sphere entry into deep glomeruli leaves fewer spheres to enter the superficial glomeruli, even when flow is equally increased in all cortical regions.

McNay et al. and others [50, 62] concluded that the use of different-sized microspheres does not affect the calculated flow distribution of either the normal or vasodilated kidney. However, Chenetz et al., Morkid et al. and Heller et al. [13, 28, 52] all reported microsphere density of the outer cortex in excess of glomerular density, a finding consistent with an artefact of geometry and skimming. Furthermore, filtration fractions obtained by estimation of glomerular plasma flow from microsphere distribution and glomerular filtration by Hannsin's technique have yielded values of 0.19 for the outer cortex, 0.41 for the middle cortex, 0.63 for the deep cortex and 0.36 for the whole rat kidney [84]. Micropuncture experiments would indicate that the filtration fractions of superficial and whole kidneys are similar in the rat. Many workers have therefore concluded that 15-μm microspheres overestimate outer cortical and underestimate inner cortical flow [7, 84].

A glomerular basement-membrane antibody as an extractable flow indicator may be a way to avoid the potential maldistribution from skimming, and/or geometric exclusion. Similar glomerular plasma flow was reported in superficial and deep glomeruli by Waldin et al. [78] using this technique in dogs. In the rat, deep glomerular flow was shown to be considerably higher than outer cortical glomerular flow with the antibody technique. There are some reservations about the use of this antibody technique. The higher specific antiserum is difficult to prepare and many investigators have failed to confirm complete extraction of the basement-membrane antibody with one pass through the kidney [41]. If it is assumed that extraction, however incomplete, is uniform throughout the cortex, the antibody distribution suggests a different relative flow distribution to the one obtained by spheres, suggesting again that the microsphere distribution is influenced by rheologic factors.

The microsphere technique is based on injection of a small volume containing radiactively labelled microspheres into the left atrium, left ventricle or possibly the

root of the aorta. It has been shown that a rapid, transient and pronounced reduction in superficial renal cortical blood flow can be elicited by injection of 1 ml plasma into the left atrium of the anaesthetised pig. This vascular response would therefore compromise the ability of the microsphere technique to accurately measure regional renal blood flow. Sandin et al. [65] examined this phenomenon using saline and microspheres and concluded that the renal vascular response to a left atrial injection is detectable as a reduction in total renal blood flow, which is most pronounced in the superficial renal cortex. Careful adjustment of the injectate temperature has failed to abolish this response [64].

Computed tomography

Radiographic methods depend on the ability of intravascularly administered contrast agents to indicate the distribution of renal cortical blood flow. Contrast agents, as compared to radioactively labelled microspheres, are in solution and therefore are not affected by steric hindrance or streaming.

By using a computed tomography scanner image to view a transverse section of the kidney, the cortical distribution of contrast agent can be measured around the entire ventral, lateral and dorsal extents of a single transverse slice of the kidney [26, 29]. This technique is limited by a number of factors, including the progressive delay between injection and the sequential scans, resulting in a gradual loss of contrast agent from the cortical region, and the need to suspend respiration for the prolonged period required. Moreover, variations in kidney position due to slight differences in breath-holding conditions may result in loss of position of adjacent slices [41].

High-speed cinematography overcomes the problem of the long sampling time [46]. Studies in phantoms have shown that iodine concentrations in tissue, as well as in blood vessels, can be reliably measured by cine-computed tomography [22, 33]. A canine study using radioactive microspheres for comparison has demonstrated that cortical blood flow may be accurately assessed by cine-computer tomography. Differences in blood flow between the renal cortex and the outer as well as the inner medulla of the dog kidney have also been demonstrated [33].

Limitations of this technique include the presence of artefacts and image noise, which may compromise the accuracy of the measured iodine concentration. The haemodynamic side effects of the contrast media are another potential source of error. Bolus injection of radiographic contrast media is thought to cause a shift in renal blood flow. Nygren et al. [54] reported an increase in cortical blood flow 2 min after the onset of infusion. A simultaneous decline in medullary blood flow was observed which was at a maximum at 10–18 min postinfusion. Using lower quantities of contrast media and completing measurements within 30 s is thought to diminish this effect. The presence of contrast medium in repeated measurements may still disturb tissue haemodynamics, thereby altering renal blood flow [34].

Positron emission tomography

Positron emission tomography (PET) permits quantitative volumetric analysis of tissue radioactivity concentrations from cross-sectional images and hence measurement of compartmental blood flow. There are several flow tracers employed for this technique, of which ^{13}N-ammonia and ^{15}O-water are the most common.

The technique assumes unidirectional transport and trapping of the ^{13}N-ammonia tracer from blood into tissue. The total nitrogen-13 activity observed in a region of interest represents the sum of activities in two functional compartments. Compartment I (C_1) contains the free nitrogen-13 ammonia in renal tissue extravascular space, while compartment II (C_2) contains the tubular bound trapped nitrogen-13 activity. Renal cortical blood flow may be calculated by solving the consequential differential equations describing each compartment, and by fitting the result to a tissue time-activity curve [53].

A similar technique for the determination of blood flow using oxygen-15 water in the kidney [32] produces a high correlation between renal blood flow estimated by ^{15}O-water and that determined by independent microsphere techniques [43]. This technique is based on a one-compartment model, where a differential equation describing the rate of change of ^{15}O-Water within the kidney is fitted to measured renal time-activity curves [53].

^{13}N-Ammonia is preferred over ^{15}O-water for renal blood flow imaging because of the better count statistics and therefore better image quality. An additional advantage is the suitability of ^{13}N-ammonia for generating parametric images of renal cortical blood flow based on Patlak graphic analysis. ^{15}O-Water is, however, metabolically inert and completely extracted in renal tissue, unlike ^{13}N-ammonia, which is not metabolically inert and has a decreasing retention fraction as renal blood flow increases above the normal range [12]. The relationship between renal blood flow and the retention fraction can be corrected for using Patlak analysis and the two-compartment model-fitting approach. There is a high degree of agreement between renal cortical blood flow estimates obtained by both ^{15}O-water and ^{13}N-ammonia. The PET approach provides evidence of the validity of ^{13}N-ammonia as a renal blood flow agent in humans.

A potential disadvantage of the ^{15}O-water technique is the need for blood volume correction for each

individual renal blood flow study. ^{15}O-Carbon monoxide has been used for blood volume correction. The fraction of radioactivity due to ^{15}O-water in the vascular spaces was removed by subtracting ^{15}O-carbon monoxide images from corresponding ^{15}O-water emission images [32]. Inaccuracies in the subtraction process are thought to cause errors, and Nitzsche et al. have therefore introduced a third parameter to the one-compartment model for ^{15}O-water in order to correct for blood volume effects [32].

Quantification of renal cortical blood flow with dynamic PET is highly reproducible. Using ^{13}N-ammonia as a tracer for PET with Patlak graphic analysis is an accurate, reproducible and rapid method for investigative and clinical applications.

Laser Doppler flow

Laser Doppler flowmeters produce a voltage signal proportional to the flux of red cells in the tissue of interest. Light of a single wave-length is guided down an optical fibre which strikes a moving red blood cell in the illuminated tissue so that its frequency is shifted in proportion to the velocity of the moving cell. This shift in frequency is converted to a voltage signal proportional to the red cell flux in the tissue. This voltage signal, which is the product of many particles, and their velocity, can be used as a quantitative index of blood flow in the different portions of the kidney. Although this technique is invasive, in that it requires the insertion of fine fibreoptic probes into the renal substance with consequent tissue disruption, it has the advantage that the zone of measurement is 1 mm beyond the fibre end and therefore not subject to disturbance. The technique also allows repeated measurements of the same area in the same animal under different experimental conditions. The exact anatomical location of the probe can be determined by subsequent dissection [27, 48].

Quantitative autoradiography

Quantitative autoradiography utilising [^{14}C]-iodoantipyrine as a tracer is based on the ^{125}I-uptake studies by Landu et al. [44] and has been used previously to measure cerebral blood flow. This technique measures the uptake of a biologically inert tracer substance in tissue. The tissue concentration of the tracer is dependent on the concentration of tracer delivered to that tissue by arterial blood flow. The theory is based on the assumption that the tracer substance mixes evenly within the renal parenchyma with no barrier to diffusion. There is, however, some controversy regarding diffusion limitations of antipyrine within tissue as discussed earlier (see radioactively labelled antipyrine).

Blood flow is measured from optical density readings calculated by an image analyser from autoradiographs of radioactive kidney slices. Blood flow is determined according to the equation first described by Skureda et al. in 1978 [63]:

$$C_t(T) = mF\ o/^T\ C_a(t)\exp\{-mF(T-t)/\lambda\}\,dt$$

where $C_t(T)$ is the mean concentration of tracer across the full width of the mucosa at time T, T is the time of death, $C_a(t)$ is the concentration of tracer in arterial blood, l is the partition coefficient of [^{14}C]-IAP between tissue and blood, F is blood flow per unit mass of tissue and m is a dimensionless parameter that expresses the degree at which the tracer attains diffusion equilibrium between tissue and blood during a capillary transit and is assumed to have a value equal to one.

Densitometric imaging has a number of limitations which originate both within the tissue and within the imaging system. System-generated random noise produced by the video cameras and digitisers may result in changes in single pixel density values on successive measurements. This noise may be minimised by the use of high-quality cameras and by image processing. Limited digital precision occurs as most imaging systems offer only 8-bit pixels in depth. That is they discriminate the entire range of densities with a sensitivity of, at best, only 1 part in 256. Therefore, the number of grey levels assigned to any portion of the calibration range is limited. This fundamental limitation to system sensitivity affects the ability to read accurate concentrations from within narrow portions of the calibration range. Limited sensor dynamic range, shading error, limited film sensitivity, non-linear media response, film noise and background variation are also problems that must be taken into consideration. These limitations, however, will result in at most a very small error which can be corrected with careful use of the image analyser.

Autoradiography has been used to measure blood flow to the gut and the ureter [31, 51]. In 1992, Geraghty and Fitzpatrick utilised this technique to measure regional renal blood flow [20]. They demonstrated marked regional differences in flow between cortex and outer and inner medullary divisions (Fig. 1). The values for regional renal blood flow reported compare well with other techniques, though they are slightly higher, suggesting that appreciable diffusion limitation of iodoantipyrine does not occur. The technique enables the investigator to compare tissue concentrations of iodoantipyrine using autoradiographs with precisely defined anatomical regions in the corresponding stained histological section. The one drawback is that this method allows focal measurements of blood flow to be performed in each animal at just one point in time. This technique also measures nutritional blood flow and, as such measures flow at the site of exchange vessels, the major advantage of this technique over conventional methods is the ability to measure flow in a precisely defined anatomical location with a resolution of 100 μm. This will enable new insight to

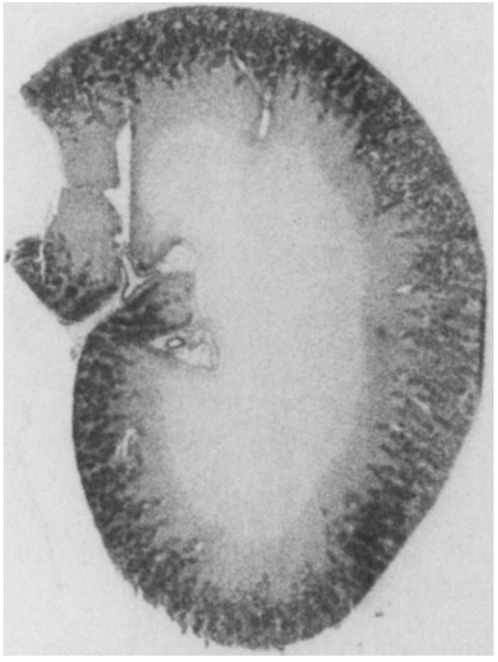

Fig. 1 Autoradiograph of a control kidney

be gained into postglomerular and peritubular flow patterns in both resting and disease states.

Conclusion

The number of techniques currently used for the determination of regional renal blood flow is a reflection of the difficulty in obtaining accurate and reproducible measurements of regional flow within the organ. Though there are still many unanswered methodological problems, advances in imaging and analytical technology, in particular the development of autoradiography has improved our understanding of the dynamics of blood flow within the kidney.

References

1. Archie JP, Fixler DE, Ullyat DJ, Hoffmann JIE, Utley JR, Carlson EL (1973) Measurement of cardiac output with organ trapping of radioactive microspheres. J Appl Physiol 35:148
2. Arendshorst WJ, Finn WF, Gottschalk CW (1976) Micropuncture study of acute renal failure following temporary renal ischemia in the rat. Kidney Int 10:S17
3. Aukland K (1967) Renal medullary heat clearance in the dog. Circ Res 20:194
4. Aukland K (1976) Renal blood flow. In: Thurau K (ed) Kidney and urinary tract physiology II. University Park Press, Baltimore, MD, pp 23–79
5. Aukland K (1980) Methods for measuring renal blood flow: total flow and regional distribution. Ann Rev Physiol 42:543
6. Aukland K, Berliner RW (1964) Renal medullary countercurrent system studied with hydrogen gas. Circ Res 4:430
7. Bankir L, Tan MM, Grunfeild J-P (1979) Measurement of glomerular blood flow in rabbits and rats: erroneous findings with 15 μm microspheres. Kidney Int 15:126
8. Bolme P, Edwell L (1970) Disappearance of xenon-133 and iodine-125 from skeletal muscle of the anaesthetised dog during sympathetic cholinergic vasodilation. Acta Physiol Scand 78:28
9. Carriere S (1970) A comparison of the disappearance curves of xenon-133 and krypton-85 for measurement of the intrarenal distribution of blood flow. Can J Physiol Pharmacol 48:834
10. Casellas D, Mimram A (1980) Influence of microsphere size upon their intrarenal distribution of the rat. 4th international symposium of radionuclides and nephrology, Stuttgart, 1980, p 124
11. Chedru M-F, Baethke R, Oken DE (1972) Renal cortical blood flow and glomerular filtration in myohemoglobinuric acute renal failure. Kidney Int 1:232
12. Chen BC, Germano G, Huang SC, et al (1992) A new noninvasive quantification of renal blood flow with N-13 ammonia, dynamic positron emission tomography and a two-compartment model. J Am Soc Nephrol 3:1295
13. Chenitz WR, Nevins BA, Hollenberg NK (1976) Preglomerular resistance and glomerular perfusion in the rat and dog. Am J Physiol 231:961
14. Clausen G, Hope A, Kirkebo A, Tyessebotn I, Aukland K (1977) Effect of vasodilation on distribution of microspheres and on zonal blood flow measured with diffusible indicators in the dog kidney. Proc Int Union Physiol Sci 13:141
15. Clausen G, Hope A, Kirkebo A, Tyessebotn I, Aukland K (1978) Glomerular versus postglomerular capillary blood flow. Abstr 7th Int Congr Nephrol Montreal: F12
16. Claussen G, Hope A, Kerkebo A, Yssenbotn T, Aukland K (1979) Distribution of blood flow in the dog kidney. I. Saturation rates for inert diffusible tracers, 125-iodoantipyrine and tritiated water, versus uptake of microspheres under control conditions. Acta Physiol Scand 107:69
17. Coelho JB (1977) Medullary plasma flows and juxtamedullary glomeruli (JMG) filtration fraction (FF) in the rat kidney. Kidney Int 12:553
18. Eckman WW, Phair RD, Fenstermacher JD, Patlak CS, Kennedy C, Sokoloff L (1975) Permeability limitation in estimation of local brain blood flow with C-14 antipyrine. Am J Physiol 229:215
19. Eklof B, Lassen NA, Nilsson L, Norberg K, Siesjo BK, Torlof P (1974) Regional cerebral blood flow in the rat measured by the tissue sampling technique: a critical evaluation using four indicators. C-14 antipyrine, C-14 ethanol, H-3 water and xenon-133. Acta Physiol Scand 91:1
20. Geraghty J, Nusubuga M, Angerson WJ, Williams NM, Saragen NN, Dervin PA, Fitzpatrick JM (1993) A study of regional distribution of renal blood flow using quantitative autoradiography. Am J Physiol 263:958
21. Goldblastt H, Lynch J, Hanzal RF, Summerville WW (1934) Studies on experimental hypertension. I. The production of persistent elevation of systolic blood pressure by means of renal ischaemia. J Exp Med 59:347
22. Gould RG, Cogan MG, Siever RS, Lipton MJ (1987) Cine-CT measurement of cortical renal blood flow. J Comput Assit Tomogr 11:779
23. Grangsjo G (1968) Variations in cortical and medullary blood flow through the dog kidney measured with heated thermocouples. Akademisk Maskinskrift, Sweden
24. Grayson J (1952) Internal calorimetry in the determination of thermal conductivity and blood flow. J Physiol (London) 118:54
25. Harsing L, Pelley K (1965) Die Bestimmug der Nierenmarkdurchblutung auf Grand der Ablagerung und Verteilung von 86-Rb. Pflugers Arch 285:302
26. Hegedus V, Faarup P (1972) Cortical volume of the normal human kidney. Correlated angiographic and morphologic investigations. Acta Radiol 12:481
27. Hellberg PO, Kallskog O, Wolgast M (1991) Red cell trapping and postischaemic renal blood flow. Differences between the cortex, outer and inner medulla. Kidney Int 40:625

28. Heller J, Horacek V, Kasalicky J (1979) Renal blood flow distribution at varying perfusion pressure in the alloperfused dog kidney. Pfluegers Arch 382:91
29. Heymsfield SB, Fulenwider T, Nordlinger B, Barlow R, Sones P, Kutner M (1979) Accurate measurement of liver, kidney and spleen volume and mass by computerised axial tomography. Ann Intern Med 90:185
30. Hope A, Clausen G, Aukland K (1976) Intrarenal distribution of blood flow in rats determined by I-125-iodoantipyrine uptake. Circ Res 39:362
31. Hudson D, Scremin OU, Guth PH (1985) Measurements of regional gastroduodenal blood flow with iodo(^{14}C)antipyrine autoradiography. Am J Physiol 248:G539
32. Inab T, Yamashita M, Kawase Y, Nakahsahi H, Watanabe H (1989) Quantitative measurement of renal plasma flow by positron emission tomography with oxygen-15 water. Tohoku J Exp Med 159:283
33. Jaschke W, Cogan MG, Sievers RS, Gould RG, Lipton MJ (1987) Measurement of renal blood flow by cine computed tomography. Kidney Int 31:1038
34. Jaschke W, Sievers RS, Lipton MJ, Coogan MG (1989) Cine-computed tomography assessment of regional renal blood flow. Acta Radiol 31:77
35. Kallskog O, Lindbom LO, Ulfendahl HR, Wolgast M (1975) Regional and single glomerular blood flow in the rat kidney prepared for micropuncture. Acta Physiol 94:145
36. Karlberg L, Kallskog O, Ojteg G, Wolgast M (1982) Renal medullary blood flow studied with the 86-Rb extraction method. Acta Physiol Scand 115:11
37. Katz M, Blantz R, Rector F, Seldin D (1971) Measurement of intrarenal blood flow. I. Analysis of microsphere method. Am J Physiol 220:1903
38. Keer JS (1956) Effects of complete urethral obstruction in dogs on kidney function. Am J Physiol 184:521
39. Kety S (1960) Measurement of local blood flow by the exchange of an inert, diffusible substance. Meth Med Res 8:228
40. Kety SS (1951) The theory and applications of the exchange of inert gas at the lungs and tissues. Pharmacol Rev 3:1
41. Knox FG, Ritman EL, Romero JC (1984) Intrarenal distribution of blood flow. Evolution of a new approach to measurement. Int Soc Nephrology 2:473
42. Knox FG, Spielman WS (1983) Renal circulation. American Physiological Society, Washington, DC, p 183
43. Kuten A, Roval HD, Griffeth LK, Mintum MA, Perez CA, Wassweman TH, Ter-Pogossian MM (1992) Positron emission tomography in the study of acute radiation effects on renal blood flow in dogs. Int Urol Nephrol 24:527
44. Landu WM, Freygang WH, Roland LP, Sokoloff L, Kety SS (1955) The local circulation of the living brain; values in the unanesthetized and anethetised cat. Trans Am Neurol Assoc 80:125
45. Lassen NA, Longley JB (1961) Countercurrent exchange in vessels of renal medulla. Proc Soc Exp Biol Med 106:743
46. Lipton MJ, Byod DP, Cann C, Strauss L, Sievers RS (1985) Attenuation changes of the normal and ischaemic canine kidney. Dynamic CT scanning after intravenous contrast medium bolus. Acta Radiol Diagnosis 26:321
47. Lote C (1987) Principles of renal physiology, 2nd edn. Croom Helm, London p 86
48. Mattson DL, Lu S, Roman RJ, Crowley AW (1993) Relationship between renal perfusion pressure and blood flow in different regions of the kidney. Am J Physiol 33:R578
49. Mauer SM, Steffes MW, Ellis EN, Sutherland DER, Brown DM, Gotez FC (1984) Structural-functional relationships in diabetic nephrectomy. J Clin Invest 74:1143
50. McNay JL, Abe Y (1970) Pressure dependent heterogeneity of renal cortical blood flow in dogs. Circ Res 27:571
51. Mooney E, Geraghty J, O'Connell M, Kent P, Quarieschi A, Sarazen A, Fitzpatrick J (1994) Radiotracer measurement of ureteric blood flow. J Urol 152:1022
52. Morkid L, Ofstad J, Willassen Y (1978) Diameter of afferent arterioles during autoregulation estimated from microspheres. Data in the dog kidney. Circ Res 42:181
53. Nitzsche EU, Choi Y, Killion D, et al (1993) Quantification and parametric imaging of renal cortical blood flow in vivo based on Patlak graphical analysis. Kidney Int 44:985
54. Nygren A, Ulfendahl JR, Hansell P, Erikson U (1988) Effects of intravenous contrast medium on cortical and medullary blood flow in rat kidney. Invest Radiol 23:753
55. O'Dorisio TM, Stein JH, Osgood RW, Ferris TF (1973) Absence of aglomerular blood flow during renal vasodilation and hemorrhage in the dog. Proc Soc Exp Biol Med 31:277
56. Olivetti G, Anversa P, Rigamonti W, Vitali-Mazza L, Loud AV (1977) Morphometry of the renal corpuscle during normal postnatal growth and compensatory hypertrophy. J Cell Biol 75:573
57. Pabico RC, McKenna BA, Freeman RB (1975) Renal function before and after unilateral nephrectomy in renal donors. Kidney Int 8:166
58. Passmore JC, Neiberger RE, Eden SW (1977) Measurement of intrarenal anatomic distribution of krypton-85 in endotoxic shock in dogs. Am J Physiol 232(1): H54
59. Rasmussen SN (1978) Red cell and plasma volume flows to the inner medulla of the rat kidney. Pfluegers Arch 375:291
60. Roed A, Aukland K (1969) Countercurrent exchange of heat in the dog kidney. Circ Res 25:617
61. Rosivall L, Hope A, Clausen G (1981) Incomplete and flow dependent extraction of 86-Rb in the rat. Pflugers Arch 390:216
62. Rueda G (1978) Distribution of microspheres of 15 ± 5 μm diameter in dog kidneys. Experientia 35:617
63. Sakurada OC, Kennedy J, Jehle JD, Carbin GL, Sokoloff L (1978) Measurements of local cerebral blood flow with (14C)antipyrine. Am J Physiol 227:816
64. Sandin R, Feuk U, Modig J (1990) Disturbances in renal cortical perfusion with reference to the microsphere technique. Acta Anaesthesiol Scand 34:457
65. Sandin R, Feuk U, Modig J (1993) Renal vascular response to left atrial injection. An experimental study in the pig. Acta Anaesthesiol Scand 37(1):60
66. Sapirstein LA (1956) Fractionation of the cardiac output of rats with isotopic potassium. Circ Res 4:689
67. Schmitz-Feuerhake I, Falkenreck-Herbst I, Coburg AJ, Wonigkeit K, Gerhardt K, Prevot H (1978) Atraumatic method of renal blood flow estimation by xenon-133 inhalation and its application to transplanted kidneys. Eur J Clin Invest 8:75
68. Stein J (1976) The renal circulation. In: Brenner BM, Rector FC (eds) The kidney. Saunders, Philadelphia, p 215
69. Stein J, Boonjarern S, Wilson CB, Ferris TF (1973) Alterations in intrarenal blood flow distribution. Methods of measurements and relationships to sodium balance. Circ Res 32:61
70. Stein JH, Ferris TF, Juprich JE, et al (1971) Effect of renal vasodilation on the distribution of cortical blood flow in the kidney of the dog. J Clin Invest 50:1429
71. Steiner SH, King RD (1970) Nutrient renal blood flow and its distribution in the unanesthetised dog. J Surg Res 10:133
72. Thornburn GD, Kopald HH, Herd JA, Hollenberg M, O'Morchoe CCC, Burger AC (1963) Intrarenal distribution of nutrient blood flow determined with 85Kr in the unanesthetized dog. Circ Res 12:290
73. Thurau K, Sugiura T, Lilienfeild LS (1960) Micropuncture of renal vasa recta in hydropenic hamsters. Clin Res 8:383
74. Trueta J, Barclay AE, Daniel PM, Franklin KJ, Prichard MML (1948) Studies on the renal circulation. Oxford UK, 1948:128
75. Tyssebotn I, Kirkebo A (1979) Renal cortical blood flow distribution measured by hydrogen clearance during dopamine and acetylcholine infusion. Effect of electrode thickness and position in cortex. Acta Physiol Scand 106:385
76. Vaughan ED, Sorenson EJ, Gillenwater JY (1970) Renal haemodynamic response to chronic unilateral ureteric obstruction. Surg Form 19:536

77. Wagner HN, Rhodes BA, Sasaki Y, Ryan JP (1969) Studies of the circulation with radioactive microspheres. Invest Radiol 4:374
78. Wallin JD, Rector FC, Seldin DW (1971) Measurement of intrarenal plasma flow with antiglomerular basement membrane antibody. Am J Physiol 221:1621
79. Wilde WS, Thurau K, Schnermann K, Prchal K (1963) Counter current multiplier for albumin in renal papilla. Pflugers Arch Ges Physiol 278:43
80. Wise KL, McCann RL, Dunnick NR, Paulson DF (1988) Renovascular hypertension. J Urol 140:911
81. Wolgast M (1968) Studies on the regional renal blood flow with 32-P labelled red cells and small beta-sensitive semiconductor detectors. Acta Physiol Scand (Suppl) 313:
82. Wolgast M (1972) Renal medullary red cell and plasma flow as studied with labelled indicators and internal detection. Acta Physiol Scand 88:215
83. Wolgast M, Karlberg L, Kullskog A, Norlen BJ, Nygien K, Ojtey G (1982) Haemodynamic alterations in ischaemic acute renal failure. Nephron 31:301
84. Yarger WE, Byod MA, W SN (1978) Evaluation of methods of measuring glomerular and nutrient blood flow in rat kidneys. Am J Physiol 235:H592
85. Zillig B, Schuler G, Truniger B (1978) Renal function and intrarenal hemodynamics in acutely hypoxic and hypercapnic rats. Kidney Int 14:58